SEISMIC BEHAVIOR OF CONCRETE COLUMN REINFORCED WITH ULTRA-HIGH STRENGTH REBARS UNDER DYNAMIC LOADING

T. Takeuchi[(1)], Y. Sun[(2)], P.B. Shing[(3)]

[(1)] *Assistant Professor, Graduate School of Engineering, Kobe Univ., Japan, takeuchi_t@person.kobe-u.ac.jp*
[(2)] *Professor, Graduate School of Engineering, Kobe Univ., Japan, sun@person.kobe-u.ac.jp*
[(3)] *Professor, Dept. of Structural Engineering, Univ. of California, San Diego, pshing@ucsd.edu*

Abstract

As building codes have been advanced to ensure life safety, more attention has been dedicated to minimizing economic losses and maintaining the serviceability of buildings after strong earthquakes. To this end, the authors have proposed the use of ultra-high-strength rebars having a low bond strength (referred to as SBPDN rebar) as longitudinal reinforcement for concrete columns, and have verified with quasi-static tests that these columns can exhibit a stable response and a significantly reduced residual deformation up to a large lateral drift level. The good behavior of the columns can be attributed to the low bond strength, which reduced the plastic deformation of the rebars by spreading the steel strain over a longer region.

This paper presents an investigation of the seismic performance of columns reinforced with SBPDN rebars under dynamic lateral loading. Five cantilever columns of 1/3 scale were fabricated and tested under a constant axial compression with axial load ratio of 20%. All the columns had a 250-by-250 mm cross section and a shear-span ratio of 3.0. The variables investigated were the type of longitudinal rebars and the lateral load histories. Three specimens were longitudinally reinforced with SBPDN rebars having a yield strength of 1361 MPa, while the other two were reinforced with normal strength deformed rebars having a yield strength of 391 MPa for comparison purpose. Four of the five specimens were tested under fully reversed displacement cycles with increasing amplitudes. Two of the four specimens were tested under a quasi-static condition, and the other two were tested with a constant lateral displacement rate of 0.04 rad./s in terms of the drift angle. The fifth one, which had SBPDN rebars, was subjected to real-time pseudo-dynamic loading.

The hysteretic load-displacement curves for the specimens subjected to fully reversed lateral displacement cycles under the high displacement rate were similar to those for specimens that were tested under quasi-static loads. The envelopes of the hysteresis curves for the specimens subjected to dynamic loading show a slightly higher resistance than those obtained with quasi-static loads due to the strain-rate effect. All the columns reinforced with SBPDN rebars showed stable hysteresis curves with low residual deformation despite the loading history. It is concluded that concrete columns reinforced with SBPDN rebars behaved in the same way under quasi-static and dynamic loads.

Keywords: residual deformation; bond-slip; drift rate; real-time pseudo-dynamic loading

1. Introduction

After several recent strong earthquakes, most of buildings designed in accordance with the current building codes kept the secure without collapse, but some of them had a large residual deformation, which may prevent the damaged city from the swift restoration. Therefore, more attention has recently been dedicated to minimizing economic losses and maintaining the serviceability of buildings after strong earthquakes.

To this end, the authors have proposed the use of ultra-high-strength bars having a low bond strength (referred to as SBPDN bar) as longitudinal reinforcement for concrete columns, and have verified with quasi-static tests that these columns can exhibit a stable response and a significantly reduced residual deformation up to a large lateral drift level [1-3]. In the proposed method, the SBPDN bar are used to delay the yielding of longitudinal bars, avoid concentration of steel strain within the so-called plastic hinge regions, and reduce the residual deformation, rather than to decrease construction cost and reinforcement congestion. The effectiveness of the SBPDN rebar, however, have not been investigated in the column under dynamic lateral loading.

This paper presents an investigation of the seismic performance of columns reinforced with SBPDN bars under dynamic lateral loading. Five cantilever columns of 1/3 scale were fabricated and tested under a constant axial compressive load ratio of 20%. The variables investigated were the type of longitudinal rebars and the lateral load histories. Three specimens were longitudinally reinforced with SBPDN bars having a yield strength of 1361 MPa, while the other two were reinforced with normal strength deformed rebars having a yield strength of 391 MPa for comparison purpose. Four of the five specimens were tested under fully reversed displacement cycles with increasing amplitudes. Two of the four specimens were tested under a quasi-static condition, and the other two were tested with a constant lateral displacement rate of 0.04 rad./s in terms of the drift angle. The fifth one, which had SBPDN rebars, was subjected to real-time pseudo-dynamic loading.

2. Outlines of experiment

2.1 Details of specimens

Figure 1 shows the dimensions and reinforcement details of the five cantilever columns, and Table 1 lists their design parameters. The mechanical properties of the steel bars used are summarized in Table 2.

All the columns had a 250-by-250 mm square cross section and a shear-span ratio of 3.0 and were transversely reinforced by D6 deformed bars spaced at 30 mm on center. Ready mixed concrete made of

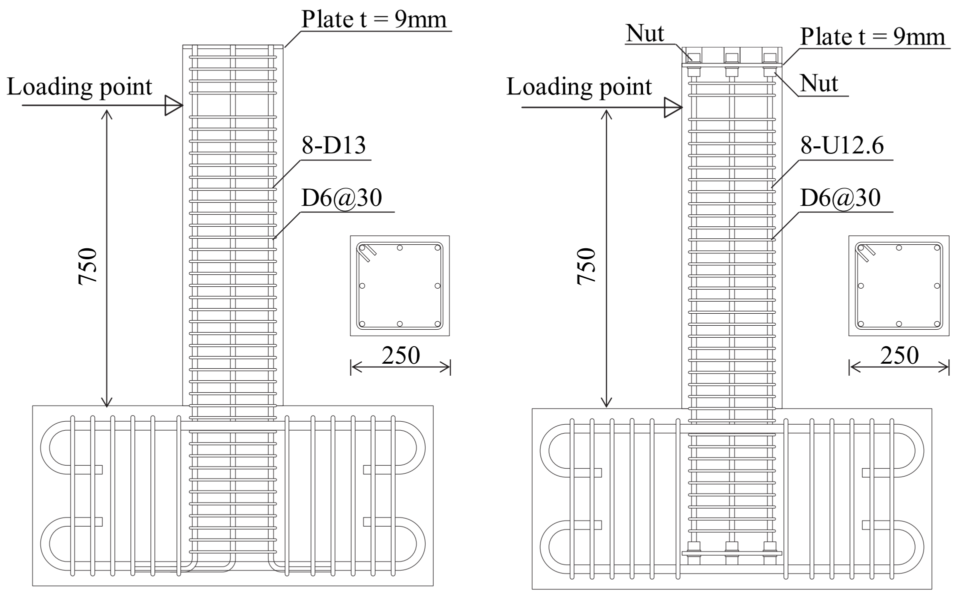

(a) RC-S/RC-D (b) HRC-S/HRC-D/HRC-H

Fig. 1– Dimensions and reinforcement details of test columns

Portland cement and coarse aggregates with maximum diameter of 20 mm was used to fabricate the specimens. Three specimens were longitudinally reinforced with eight SBPDN bars (U12.6), while the other two were reinforced with eight normal strength deformed rebars (D13). Each SBPDN bar had had screw threads at both ends and was anchored to a steel plate by nuts. One end of the D13 bar was welded to a steel plate, while the other end was anchored with a 90° hook.

2.2 Test setup

A schematic view of the test setup is presented in Fig. 2. Each specimen was fixed to the strong floor and tested under lateral loading and constant axial compression. The axial compression with an axial load ratio of 0.2 was applied with two φ26 PC tendons located 450mm north and south from the center of the column-section. However, the applied axial force could not be controlled during lateral loading, and fluctuated between axial

Table 1 – Primary experimental parameters and main test results

Specimen	f'_c (MPa)	P (kN)	Longitudinal rebars type	Loading program	Q_{exp} (kN)	R_{exp} (%)
RC-S	43.5	543.8	8-D13	Reversed cyclic load in quasi-static	119.2	1.30
RC-D	41.9	523.8	(ρ_g = 1.62%)	Reversed cyclic load with a constant drift rate	126.3	1.01
HRC-S	42.9	536.3	8-U12.6	Reversed cyclic load in quasi-static	139.9	3.94
HRC-D	43.0	537.5	(ρ_g = 1.60%)	Reversed cyclic load with a constant drift rate	147.8	3.95
HRC-H	45.0	562.5		Real-time pseudo-dynamic loading	148.5	3.24

Note: f'_c = concrete cylinder strength; P = axial force; ρ_g = the steel ratio of longitudinal rebar; Q_{exp} = ultimate lateral load; R_{exp} = drift angle at Q_{exp}.

Table 2 – Mechanical properties of the steels

Name	Type	A_s (mm^2)	f_y (MPa)	f_u (MPa)	ε_y (%)	φ (%)	E_s (GPa)
D6	SD295A	31.67	377	513	0.20	19.0	193
D13	SD345	126.7	391	564	0.22	17.8	175
U12.6	SBPDN 1275/1420	125	1362*	1469	0.84*	10.0	211

Note: A_s = nominal area; f_y = yield strength; f_u = tensile strength; ε_y = yield strain; φ = elongation ratio; E_s = Young's modulus; * = 0.2% offset yield strength and strain corresponding to the strength.

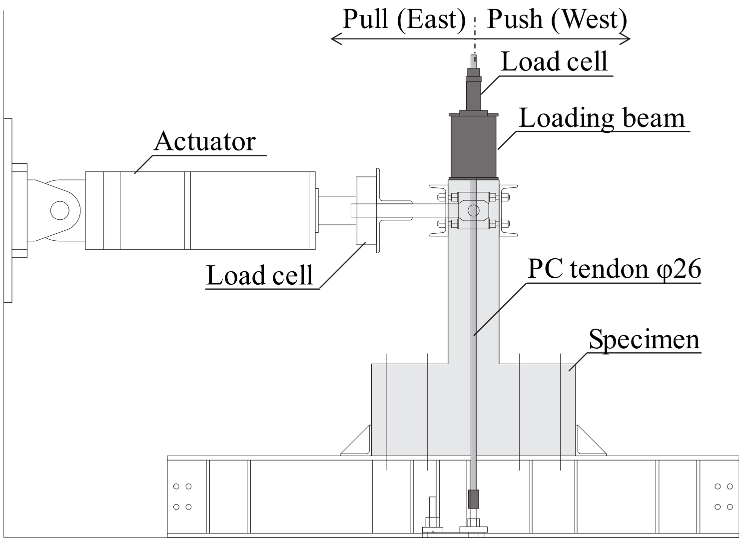

Fig 2 – Schematic view of test apparatus load ratios of 0.19 and 0.23. The hydraulic actuator with capacity of 400kN in pulling and pushing was used to apply t he lateral force.

One displacement transducer (DT) was installed to measure the lateral displacement at the loading point and four DTs were installed to measure the local axial displacement within the end 1D and 2D regions of the specimens. Strain gauges were attached on two longitudinal bars located on the extreme tension and compression sides of the column section at several heights.

2.3 Loading program for reversed cyclic lateral loading

Four of the five specimens were tested under fully reversed displacement cycles with increasing amplitudes. The cyclical lateral force was controlled by drift ratio (R), which is the ratio of the measured lateral displacement to the shear span. The loading program is illustrated in Fig. 3(a). Two of the four specimens were tested under a quasi-static condition, and the other two were tested with a constant lateral displacement rate of 0.04 rad./s in terms of the drift angle, as shown in Fig. 3(b). The damage of the columns subjected to the quasi-

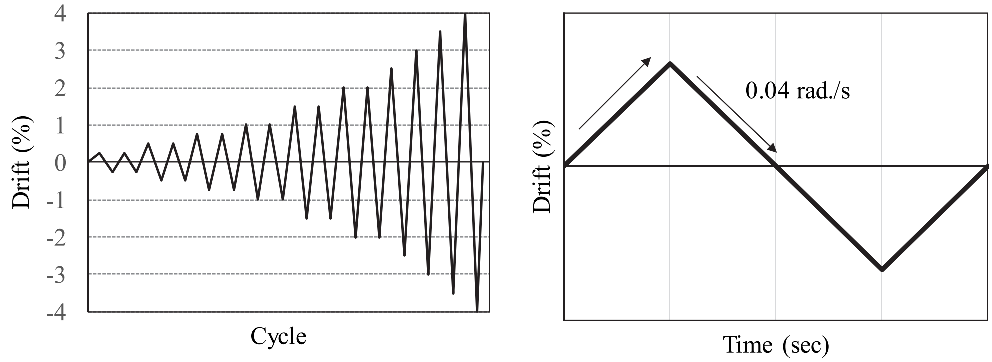

(a) Loading program

(b) Time history of drift with a displacement rate in each cycle

Fig 3 –Cyclic lateral loading program

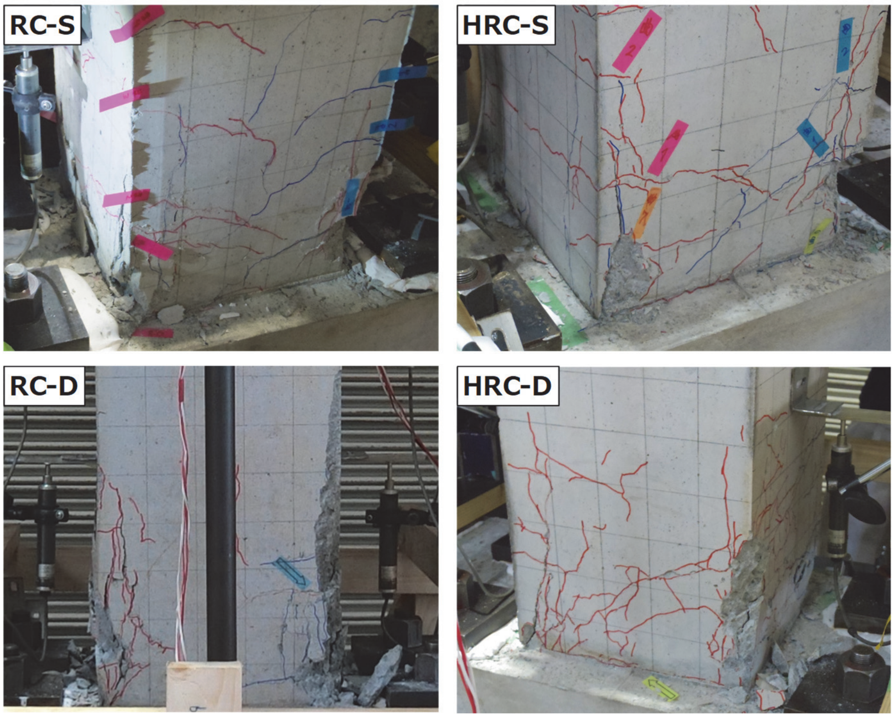

Fig 4 –Damage states at drift of 3%

static lateral load was observed when the drift reached peak drifts and zero, while that of the column under the dynamic lateral load was observed after each cycle.

3. Experimental results and discussions for cyclic lateral loading

Damage states observed at R = 3 % are shown in Fig. 4. The specimens showed similar damage with several flexural cracks and the spalling off of the cover concrete at compressive region near the column base. The damages of the columns concentrated within the end region of about 200mm in length regardless the type of rebar and the drift rate of lateral loading. For the two specimens RC-S and RC-D reinforced with normal-strength D13 bars, the strain of the longitudinal bars reached their yield strain at R = 1.0%, while no SBPDN bars in the other specimens yielded until the end of testing.

The measured lateral force-drift ratio relationships of four specimens subjected to the cyclic lateral loading are shown in Fig. 5. The horizontal component of the load applied by the PT tendons was subtracted from the measured lateral force. The blue lines shown in Fig. 5 represent the strength decline caused by the P-δ effect. The specimens reinforced by normal-strength D13 bars exhibited typical ductile behavior up to R = 4%. Specimens RC-S and RC-D reached their maximum load-carrying capacities at R = 1.3% and 1.0%, respectively. Subsequently, the lateral resistance of each specimen degraded nearly in accordance with the P-δ effect while absorbing the energy with the rebar yielding.

Both of the specimens reinforced with SBPDN bars exhibited very stable cyclical behavior and a mild hardening post-yield behavior until R = 4% while the increase in lateral resistance began to get mild at about R = 1% due to the softening of concrete. Both specimens had a narrow hysteresis loop and small residual deformation because their longitudinal bars did not yield.

Figure 6 shows comparisons of the average envelope curves in pull and push direction in terms of the relationship between the lateral force and the drift ratio. This figure indicates that the lateral resistance of the specimen subjected to the lateral load with a drift rate of 0.04rad./s was higher than that of the specimen

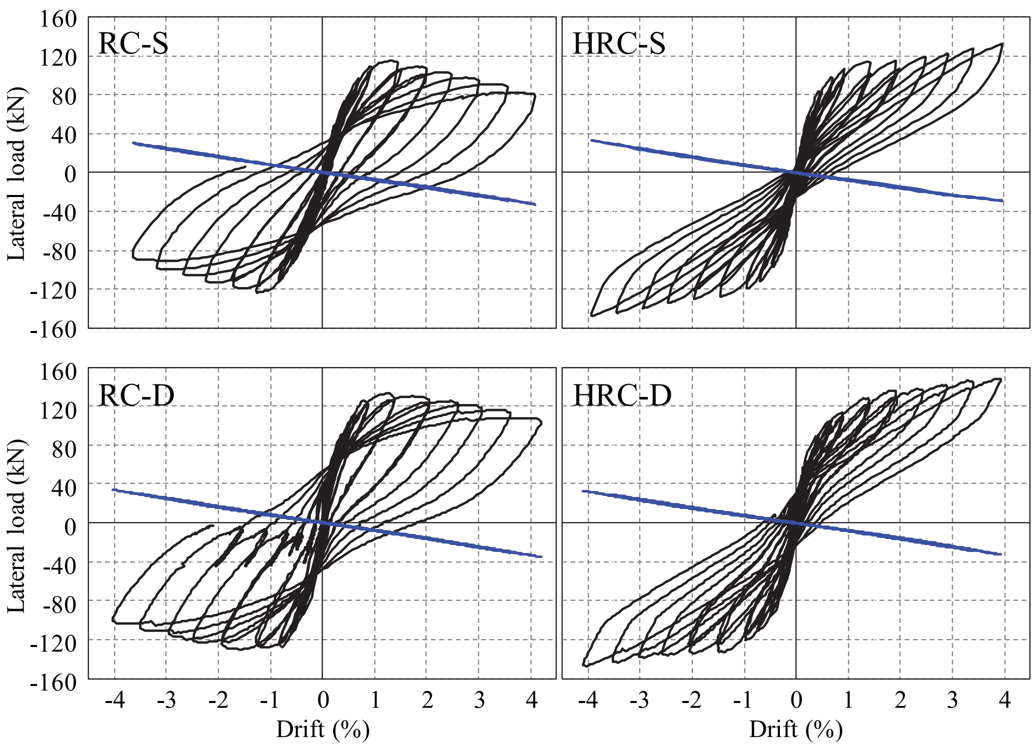

Fig 5 – Lateral force versus drift ratio curves subjected to the quasi-static lateral load. This could be attributed to the increase in the material strength with the strain rate [4-5].

Figure 7 compares the measured residual drift ratios. After R = 1%, a sharp increase in the residual drift was observed for the specimens reinforced with normal-strength D13 bars because of the yielding of the longitudinal bars. The specimens reinforced with SBPDN bars showed much reduced residual deformations regardless of the loading rate.

Figure 8 shows the distributions of the strains in the longitudinal bars along column height at specific drift levels of the specimens. No results are plotted at several measuring points at large drifts because of the damage of the strain gauges. The strains in the longitudinal bars in the specimens with D13 bars developed within the end region of 265 mm. The strains measured from SBPDN bars developed in the same region as the

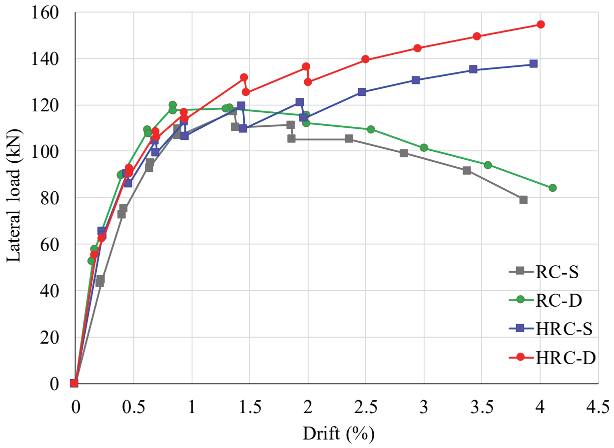

Fig 6 – Comparisons of the envelopes curves for specimens

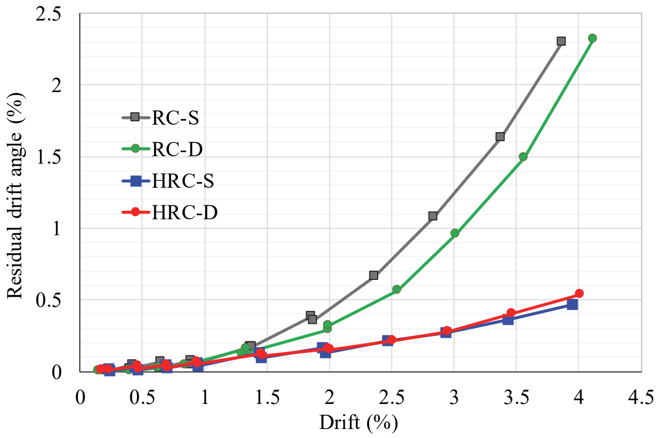

Fig 7 – Measured residual drift ratios plotted against the peak drift levels before unloading

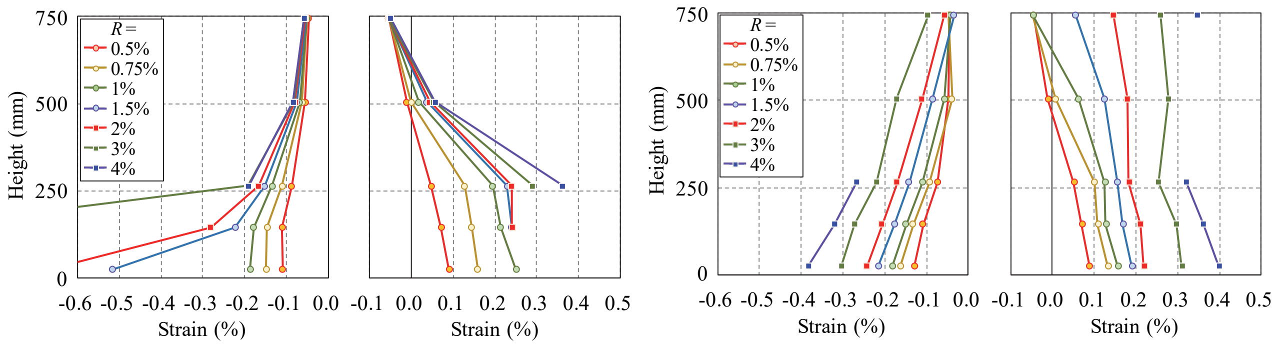

(a) RC-S (b) HRC-S

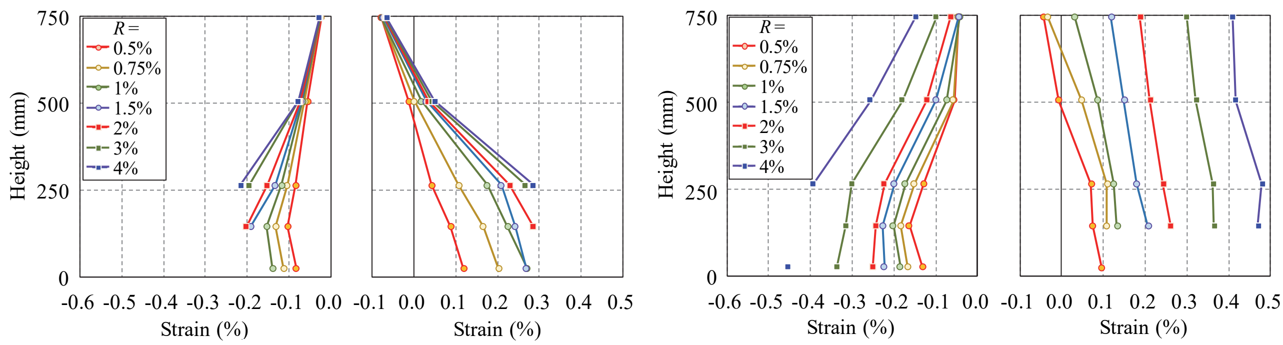

(c) RC-D (d) HRC-D

Fig 8 – Strain distributions in longitudinal reinforcement

D13 bars until R = 0.75%, but after that, show a more uniform distribution along the column elevation as the drift increased regardless of the loading rate.

4. Real-time pseudo-dynamic loading test

4.1 Loading program

Specimen HRC-H was tested with an assumption that the specimen was a part of a building subjected to earthquakes. The assumed building was a five DOF system with mass assumed to concentrate on each floor level, viscous damping and lateral stiffness of each story provided by nonlinear shear springs. The first story has two shear springs, the half part of one of which was the cantilever test specimen, and the half displacement of the first layer was transmitted to the actuator as a target displacement, and the response force of the test specimen was used as the restoring force of the spring. The weight of the mass was determined so that the axial force applied to the column of the first story was 0.2, and was equally divided into each mass. A damping ratio of 5% is assumed in the analysis, implemented using the Rayleigh damping model for the 1st and 2nd natural frequency of this system, which are 2.3 and 6.9 Hz, respectively. This model was subjected to the earthquake motions that were recorded during the Imperial Valley earthquake of 1940 (El Centro) and the Kobe earthquake of 1995 (JMA Kobe). The magnitude of the input wave was adjusted to several scales, as shown in Table 3. The time of the ground motion was scaled to 0.577 according to the similitude law that was to be applied to the columns of 1/3 scale. This paper forcused on the behavior of the test specimen.

Table 3 – Summary of main test results for specimen HRC-H

Run	Ground motion		Q_{max} (kN)		R_{max} (%)	
	Type	Scale	Pull	Push	Pull	Push
1	JMA-Kobe	16%	-73.5	103.4	-0.36	0.51
2	JMA-Kobe	30%	-117.6	123.8	-0.77	0.85
3	El Centro	150%	-124.6	132.7	-1.15	1.17
4	JMA-Kobe	50%	-136.4	116.3	-1.67	1.02
5	JMA-Kobe	75%	-143.3	138.3	-2.34	1.55
6	JMA-Kobe	100%	-144.3	142.6	-2.85	2.67
7	JMA-Kobe	120%	-142.9	152.7	-3.38	3.68
8	JMA-Kobe	130%	-142.3	152.0	-3.73	4.17

Note: Q_{max} = maximum lateral load; R_{max} = maximum drift ratio.

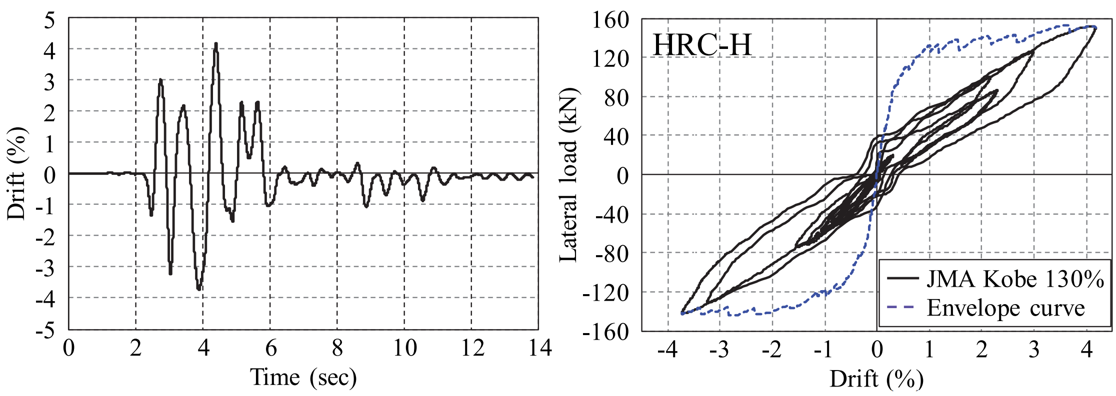

(a) Displacement response (b) Hysteresis loop

Fig 9 – Response of specimen HRC-H in the case of JMA Kobe 130%

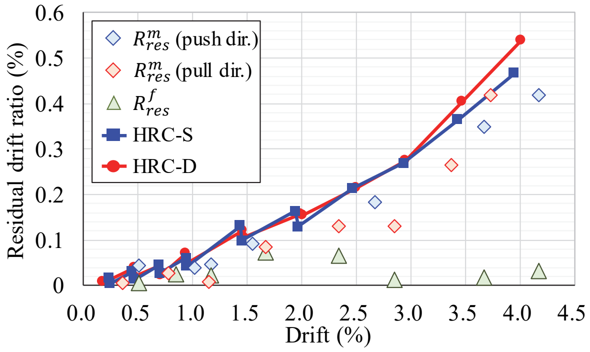

Fig 10 – Residual drift ratio of specimen HRC-H

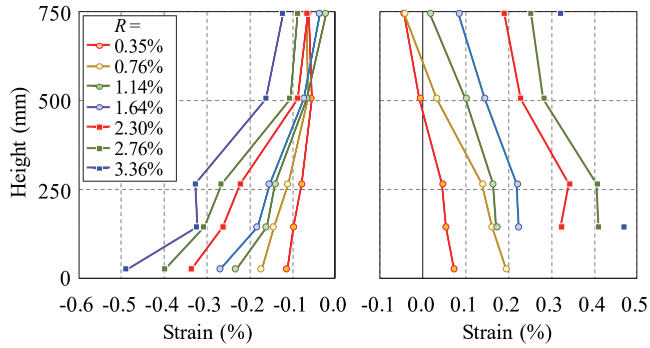

Fig 11 – Strain distributions in longitudinal reinforcement of specimen HRC-H

4.2 Experimental results and discussions

Figure 9 shows the time history of the drift ratio of specimen HRC-H and the relationship between the lateral load and drift ratio of the specimen in the case of the ground motion of JMA Kobe 130%. The blue dash line in Fig. 9(b) represents the envelope curve in terms of the relationship between the lateral force and the drift ratio for all run. Specimen HRC-H showed much reduced residual deformations as with cyclic lateral loading. This specimen exhibited a mild hardening post-yield behavior as well as the specimens with SBPDN bars under cyclic lateral loading.

Figure 10 shows maximum possible residual deformations (R^m_{res}) and final residual deformations (R^f_{res}) of specimen HRC-H. The maximum possible residual deformation (R^m_{res}) represents the residual drift after unloading from the peak drift for each ground motion, and the final residual deformation (R^f_{res}) represents the residual drift after each ground motion. The maximum possible residual deformation of specimen HRC-H was similar to the residual deformation of the specimen with SBPDN bars under cyclic lateral loading. The final residual deformation was more reduced than the maximum possible residual deformation. This could be attributed to the shake-down phenomenon [6-7].

Figure 11 shows the distributions of the strains in the longitudinal bars along column height at specific drift levels of specimen HRC-H. The strain of the SBPDN bar in specimen HRC-H developed over a long region due to the bond-slip behavior of the SBPDN bar as in cyclic lateral loading.

5. Conclution

This paper investigated the seismic performance of columns reinforced with SBPDN bars under dynamic lateral loading. Five cantilever columns were tested with variables including the type of longitudinal bars and the lateral load histories. From the experimental results presented here, the following conclusions can be drawn.

・The hysteretic load-displacement curves for the specimens subjected to fully reversed lateral displacement cycles under high displacement rate were similar to those for specimens that were tested under quasi-static loads. The envelopes of the hysteresis curves for the specimens subjected to dynamic loading show a slightly higher resistance than those obtained with quasi-static loads due to the strain-rate effect.

・All the columns reinforced with SBPDN bars showed stable hysteresis curves with low residual deformation despite the loading history. It is concluded that concrete columns reinforced with SBPDN bars behaved in the same way under quasi-static and dynamic loads.

6. Acknowledgements

This work was partially supported by JSPS Grant No. R2904 under the Program for Fostering Globally Talented Researchers. The high strength bars were provided by Neturen Co. Ltd. Their support is gratefully acknowledged. However, opinions expressed in this paper are those of the authors and do not necessarily reflect those of the sponsors.

7. References

[1] Sun Y, Takeuchi T, Funato Y, Fujinaga T (2012): Earthquake-Resisting Properties and Evaluation of High Performance Concrete Columns with Low Residual Deformation. *15th World Conference on Earthquake Engineering*, Lisbon, Portugal.

[2] Sun Y, Cai G, Takeuchi T (2013): Seismic Behavior and Performance-Based Design of Resilient Concrete Columns. *Applied Mechanics and Materials*, Vols. 438-439, 1453-1460.

[3] Sargsyan G, Cai G, Takeuchi T, Sun Y (2017): Seismic Behavior and Assessment of Drift-Hardening Concrete Columns. *16th World Conference on Earthquake Engineering*, Santiago, Chile.

[4] Scott BD. Park R, Priestley MJN (1982): Stress-Strain Behavior of Concrete Confined by Overlapping Hoops at Low and High Strain Rates. *ACI Journal Proceedings*, **79**(1), 13-27.

[5] Paulay T, Priestley MJN (1992): Seismic Design of Reinforced Concrete and Masonry Buildings, Wiley, New York.

[6] Macrae GA, Kawashima K (1997): Post-Earthquake Residual Displacements of Bilinear Oscillators. *Earthquake Engineering & Structural Dynamics*, **26**(7), 701–716.

[7] Christopoulos C, Pampanin S, Priestley MJN (2003): Performance-Based Seismic Response of Frame Structures Including Residual Deformations. Part I: Single-Degree of Freedom Systems. *Journal of Earthquake Engineering*, **7**(1), 97–118.

